Supplementary material to:

Neutralizing nanobodies against SARS-CoV-2 recognizing highly conserved epitopes at the Spike's S2 subunit

Daniel Polo-Megías[1,*], Mario Cano-Muñoz[1,a], Philipp Trolese[1,2], Sara Lestani[1,b], Ilaria La Rocchia[1,c], Andrea Pierangelini[2,d], Benedetta Fongaro[2], Patrizia Polverino de Laureto[2], Francisco J. Morales-Yánez[3,4], Jonathan Vaneyck[3,4], Alain Vanderplasschen[5], Thomas Decoville[6], Géraldine Laumond[6], M. Carmen Salinas-Garcia[1], Ana Cámara-Artigas[7], José A. Gavira[8], Christiane Moog[6,9], Mireille Dumoulin[3,4], Francisco Conejero-Lara[1,*].

[1] Departamento de Química Física, Instituto de Biotecnología y Unidad de Excelencia de Química Aplicada a Biomedicina y Medioambiente (UEQ), Facultad de Ciencias, Universidad de Granada, 18071 Granada, Spain

[2] Department of Pharmaceutical and Pharmacological Sciences, Via Marzolo 5, 30131 Padova, Italy

[3] Nano-Antibodies to Explore Protein Structure and Functions (NEPTUNS), Centre for Protein Engineering, InBios, Department of Life Sciences, University of Liège, Liège, Belgium

[4] AlpaNano, Centre for Protein Engineering, InBios, Department of Life Sciences, University of Liège, Liège, Belgium.

[5] Immunology-Vaccinology, FARAH and Faculty of Veterinary Medicine, Department of Infectious and Parasitic Diseases, University of Liège, Liège, Belgium

[6] Laboratoire d'ImmunoRhumatologie Moléculaire, Institut National de la Santé et de la Recherche Médicale (INSERM) UMR_S 1109, Institut Thématique Interdisciplinaire (ITI) de Médecine de Précision de Strasbourg, Transplantex NG, Faculté de Médecine, Fédération Hospitalo-Universitaire OMICARE, Fédération de Médecine Translationnelle de Strasbourg (FMTS), Université de Strasbourg, F-67000 Strasbourg, France

[7] Department of Chemistry and Physics, University of Almería, Agrifood Campus of International Excellence (ceiA3), Research Center for Mediterranean Intensive Agrosystems and Agri-Food Biotechnology (CIAIMBITAL), Carretera de Sacramento s/n, Almería, 04120, Spain.

[8] Laboratorio de Estudios Cristalográficos, IACT-CSIC, Armilla, 18100 Granada, Spain

[9] Vaccine Research Institute (VRI), F-94000 Créteil, France

*Corresponding authors: Daniel Polo-Megías (danielpm@ugr.es); Francisco Conejero-Lara (conejero@ugr.es).

Key words: X-ray crystallography, isothermal titration calorimetry, single-domain antibodies (sdAbs), antivirals, fusion inhibitors

[a] Present address: Department of Biotechnology and Environmental Protection, Estación Experimental del Zaidín, Consejo Superior de Investigaciones Científicas, Granada, 18008, Spain

[b] Present address: Institute for Research in Biomedicine, Università della Svizzera italiana, 6500 Bellinzona, Switzerland

[c] Present address: Department of Biomedical Sciences, University of Padua, 35131 Padova, Italy.

[d] Present address: Target Discovery Institute, Center for Medicines Discovery, Nuffield Department of Medicine, University of Oxford, Oxford, United Kingdom

Table of contents

Appendix S1. NBs selection by phage display.

For phage amplification, 1 mL of the library Joe2 was infected with the helper phage M13K07 (Thermo Fisher Scientific, Walthman, Massachusetts, USA) with a multiplicity of infection of 20 viral particles per bacterial cell. Bacteria were incubated in the presence of ampicillin (100 µg/mL) and kanamycin (70 µg/mL) overnight at 37 °C with orbital shaking. Then, the cells were centrifuged, and the soluble phages were purified from the supernatant by PEG-6000 precipitation. Three rounds (R) of panning were performed in a single well of a Multisorp 96-well ELISA plates (ThermoFisher, Walthman, Massachusetts, USA) coated with 2 µg of either the full-length HR1 mimic protein L3C or the N-terminal truncated version (N2C) overnight at 4°C. After a blocking step, the freshly precipitated phages were incubated in the well for 1 hour at room temperature to allow the binding of the phage repertoire to L3C or N2C. Then, the well was extensively washed with PBST 0.1%, and the specific phages were eluted by pH shock with 100 µl of a 1.4% solution of triethylamine and neutralized with 100 µl of Tris-HCl 100mM pH 8.

The sub-repertoires, (i.e., the eluted phages) were amplified in fresh *Escherichia coli* TG1 cells in the presence of M13KO7 helper phages as described above and used in the next round of panning. A set of 48 colonies in each round were randomly selected and stored in 2XTY media supplemented with 10% glycerol at -80°C.

For small-scale production, each clone was inoculated in 1mL of 2XTY media supplemented with ampicillin (100 µg/mL) in MASTERBLOK®, 96 wells, 2 mL deepwell plates (Greiner Bio-One Kremsmünster, Austria). The VHH production was induced by Isopropyl β-d-1-thiogalactopyranoside (IPTG) 1 mM and the cell extracts (CE) were prepared by a freeze–thaw cycle at −80 °C of the bacterial pellet and were used for ELISA screening towards the L3C or N2C protein immobilized by adsorption on 96-wells Multisorp ELISA plates.

Negative controls (i.e., wells without L3C or N2C protein) were used as blanks. Detection was performed using a mouse anti-His or a mouse anti-HA and goat anti-mouse labelled with alkaline phosphatase followed by revelation with 4-Nitrophenyl phosphate disodium (Sigma, St.Louis, Missouri, USA) for two hours and the absorbance at 405 nm was monitored using a Spectramax M2e microplate spectrophotometer (Molecular Devices, San Jose, California, USA) at 405n. Clones were considered positive if the ratio of absorbance at 405 nm between the wells coated with L3C or N2C protein and the control well was higher than 2 (panning against LC3) or higher than the average of the absorbance ratio of the negative controls plus three times the corresponding standard deviation (panning against N2C). The NBs sequences of the positive clones were classified into families according to the sequence of their CDR3 region. Thus, NBs from the same family recognize the same epitope, but their properties in terms of affinity, stability or production yield may differ due to differences in CDR1, CDR2 and framework regions.

Appendix S2. NBs' production and purification protocol.

The DNA encoding the sequence of each NB was cloned into commercial expression vectors pMECS (during the library construction) or pHEN6 (Thermo Fisher Scientific, Waltham MA), which were used to transform BL21(DE3) *E. coli* cells. After overnight incubation at 37 °C of Petri dishes seeded with the transformed cells, single colonies were obtained and used to inoculate small volumes (~10 mL) of lysogeny broth (LB) medium containing 100 µg/mL ampicillin, 1 mM $MgCl_2$, 2% (w/v) glucose. The cultures were grown overnight at 37 °C. Glycerol stocks were prepared by mixing 500 µl of each saturated NB culture with the same volume of 60% (v/v) sterile glycerol.

For each NB production, a pre-inoculum was prepared the day before using the corresponding glycerol stock as described above. The saturated pre-inoculum was then used to scale up the cultures in larger 2 L flasks containing 0.5 L of sterile terrific broth (TB) supplemented with 100 µg/mL ampicillin, 1 mM $MgCl_2$, and 0.1% (w/v) glucose. The cultures were grown at 37 °C shaking at 170–190 rpm in orbital shakers. Once the optical density (OD) reached a value of 1.2–1.5, overexpression was induced by adding 1 mM IPTG to the cultures. After overnight incubation at 27 °C, cells were harvested by centrifugation for 10 min at 6,000 rpm (4 °C) in a preparative centrifuge (Hettich Zentrifugen Roto Super, Kirchlengern, Germany) and lysed by sonication (Sonifier Model 250/450, Branson Ultrasonics, Connecticut, USA).

The soluble fraction containing the NB was then clarified by centrifugation for 30 min at 14,000 rpm (4 °C) in a bench microcentrifuge and subjected to a series of chromatographic steps as previously described by our group starting with a nickel-affinity chromatography followed by anionic or cationic exchange chromatography, depending on the isoelectric point of each NB (Table S2). For the affinity step, 5 mL His-trap FF connected to a ÄKTAprime plus FPLC system was used (GE Healthcare Bio-Sciences AB, Sweden). For anionic and cationic exchange 5 mL, Hi-Trap Q FF and Hi-Trap FF columns were employed (GE Healthcare Bio-Sciences AB, Sweden).

The purity and identity of the NBs were assessed at each step by SDS-PAGE and mass spectrometry. Pure NB aliquots were stored frozen at -80°C in 50 mM sodium phosphate, pH 7.4 buffer [1,2].

Table S1. Data collection and refinement statistics of the L3B–NB278–NB184 crystallographic structure (PDB ID: 9RN6).

L3B-NB278-NB184	
Wavelength	0.98
Resolution range	19.99 - 2.40 (2.49 - 2.40)
Space group	P 2 2_1 2_1
Unit cell	47.56 67.34 230.78 90 90 90
Total reflections	212001 (22131)
Unique reflections	29937 (3097)
Multiplicity	7.1 (7.1)
Completeness (%)	99.8 (99.9)
Mean I/sigma(I)	12.4 (1.9)
Wilson B-factor	55.75
R-merge	0.07 (1.04)
CC1/2	0.99 (0.81)
Reflections used in refinement	29858 (1511)
Reflections used for R-free	1434 (54)
R-work	0.247 (0.398)
R-free	0.263 (0.438)
Number of non-hydrogen atoms	3504
macromolecules	3504
Protein residues	454
RMS(bonds)	0.005
RMS(angles)	0.737
Ramachandran favored (%)	98.65
Ramachandran allowed (%)	1.35
Ramachandran outliers (%)	0.00
Rotamer outliers (%)	0.00
Clashscore	0.00
Average B-factor	80.50
macromolecules	80.50
Number of TLS groups	10

Values in parentheses are for highest-resolution shell.
The resolution cutoff was determined based on the CC1/2 criterion [3].

Table S2. Amino acid sequences of SARS-CoV-2 HR1-targeting NBs. The CDR1, CDR2, and CDR3 regions are respectively highlighted in orange, light blue, and red. Hemagglutinin and histidine tags are shown in blue and green, respectively. Cysteine residues are underlined. Residue differences between CDRs of NBs belonging to the same family are highlighted in bold.

	1st-gen NB sequences
NB107 (Family VI)	QVQLQESGGG LVQPGGSLRL SCKASGINLE NYAVGWFRQV PGKERERISC I**N**ILDYKEYE ESVKGRFTVS RDSAKSTVYL QMNGLKSDDT AVYYCAAEMH LRSGC**PA**GFD YWGQGTQVTV SSAAAYPYDV PDYGSHHHHH H
NB113* (Family II)	QVQLQESGGG LVEPGGSLRL SCAASGGTLS SYDMDWFRQA PGKDREFVAR ISRGPTSAYY ADSKKGRFTI SRDNAKNTVY LQMNSLKPED TGVYYCAANL YYWGQGTQVT VSSHHHHHH
NB117 (Family I)	QVQLQESGGG LVQPGGSLRL SCAAS**GF**T**LD** **D**Y**A**M**S**WFRQV PGKEREIVAA ISGTGGRTFY ADSMKGRFTI SRDNAKNTVI LQMNSLKPGD TAVYY**C**AAGR EYYEGTYYTA QEEYDVWGQG TQVTVSSAAA YPYDVPDYGS HHHHHH
NB118* (Family V)	QVQLQESGGG LVQAGGSLTL SCAASGIIFR NTAMGWDRQA PGKQRELVAT ILTGGNTVYV PSVKGRFTIS RDNDKNTVSL EMNRLTPEDT AVYYCRAYGS RASSWGQGTQ VTVSSHHHHH H
NB127 (Family IV)	QVQLQESGGG LVQAGGSLRV SCAASGRIFS TDEMGWYRQA PGKQRELVAS ITSGSRGSTR ITYADSVKGR FTISRDIAKN AVYLQMNSLK PEDTAVYYCN LNRIGYDYWG QGTQVTVSSA AAYPYDVPDY GSHHHHHH
NB248* (Family VI)	QVQLQESGGG LVQPGGSLRL SCKASGINLE NYAVGWLRQV PGKERERISC I**T**ILDYKEYE ESVKGRFTVT RDSAKNTVYL QMNGLKSDDT AVYYCAAEMH LRSGCP**GR**FD YWGQGTQVTV SSHHHHHH
NB268 (Family I)	QVQLQESGGG LVQAGGSLRL SCAAS**DR**T**FS** **K**Y**S**M**G**WFRQA PGKEREIVAA ISGTGGRTFY ADSMKGRFTI SRDNAKSTVI LQMNSLKPGD TAVYYCAAGR EYYEGTYYTA QEEYDVWGQG TQVTVSSAAA YPYDVPDYGS HHHHHH
NB278* (Family III)	QVQLQESGGG LVQAGGSLRL SCAASGIAFS NNAMGWYRQA PGKQRELVAN IITFGNTYYT DSVKGRFTIS RDNAKNTVYL QMNSLKPEDT AVYYCHTYGD SPERGYWGQG TQVTVSSHHH HHH
	2nd-gen NB sequences
NB147 (Family I)	QVQLQESGGG LVQAGASLRL SCAASGRTFS TYAMGWFRQA PGKEREFVAT IRWSGGTTYY AESVKGRFTI SRDNAKNTVY LQMNNLKPED TAVYYCALNS DTLLLTTTRA DYRGQGTQVT VSSAAAYPYD VPDYGSHHHH HH
NB184 (Family III)	QVQLQESGGG LVHPGQSLTL SCAPSGRTFS NYDIGWFRQA PGKEREFVAD IRLNSGSTYY ADSVKGRFTI SRDNVKNTVY LQMNSLKPED TAVYYCAARS PGGILYDYWG QGTQVTVSSA AAYPYDVPDY GSHHHHHH
NB235 (Family II)	QVQLQESGGG LVQAGASLRL SCAASGRTFS TYAMGWFRQA PGKEREFVAT IRWSGGTTYY AESVKGRFTI SRDNAKNTVY LQMNNLKPED TAVYYCALNN DTLLLTTTRA DYRGQGTQVT VSSAAAYPYD VPDYGSHHHH HH

(*) Sequence of NBs recloned in pHEN6 expression vector.

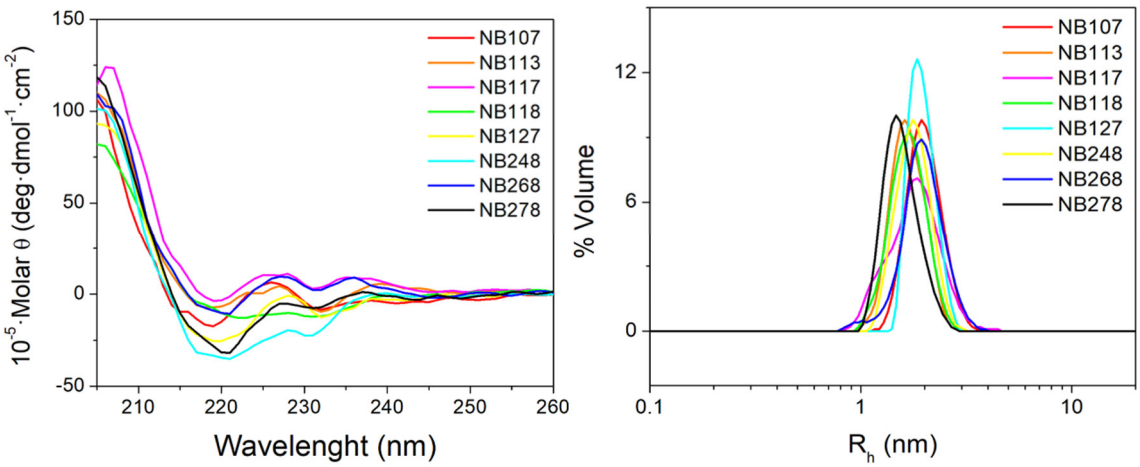

Figure S1. 1st-gen NBs far-UV circular dichroism (CD) spectra (left) and hydrodynamic radius (R_h) distributions obtained by dynamic light scattering (DLS) (right). Experiments were carried out at 25 °C in 50 mM phosphate buffer (pH 7.4) and a protein concentration of 25 µM. All NBs showed a CD spectrum typical of β-sheet-rich proteins and R_h values between 1.5 and 1.9 nm, consistent with a monomeric state of the molecules.

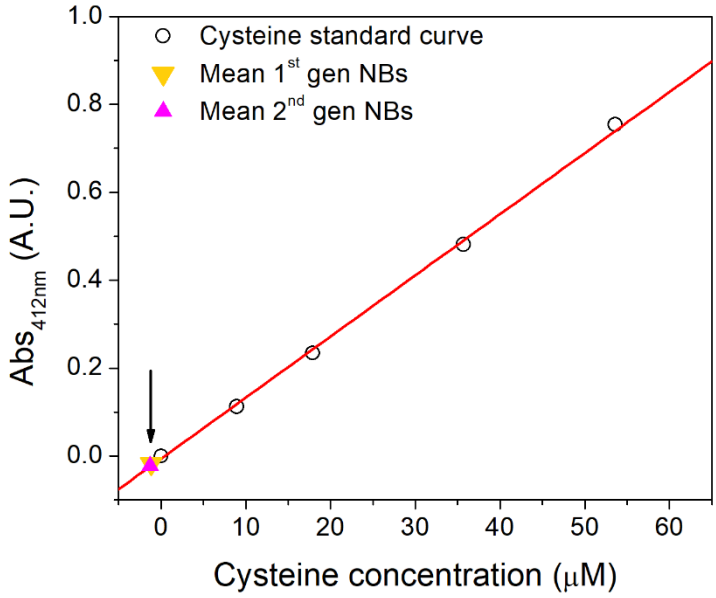

Figure S2. Quantification of sulfhydryl groups (SH_2^-) in 1st- and 2nd-gen NBs using Ellman's reagent. All NBs showed no evidence of reduced cysteines, indicating that a disulfide bond had formed between the FR1 and FR2 in NB113, NB117, NB118, NB127, NB268, NB278, NB147, NB184, and NB235. The additional disulfide bridge between FR2 and CDR3 had also formed in NB107 and NB248. The experiment was carried out in 50 mM phosphate buffer (pH 7.4) containing 5 mM EDTA. A cysteine solution at the indicated concentrations was used as standard. The red line represents the linear fit of the standard experimental data, with a R^2= 0.99.

Appendix S3. Quantification protocol of Sulfhydryl groups (SH_2^-) using Ellman's reagent.

The quantification of the SH^- groups was performed as described by Parody *et al*. [4] and following the instructions provided by Thermo Scientific (Product No. 22582, available online at: http://www.thermoscientific.com/pierce). Briefly, a fresh stock solution of cysteine was prepared at 1 mM by dissolving the necessary amount of reagent in 50 mM sodium phosphate buffer (pH 7.4) containing 2 mM EDTA. DTNB solution was prepared at 10 mM at the same buffer. In this case, additional pH adjustment with NaOH was required.

Cysteine standard solutions were prepared from the initial stock ranging from 0 to 1 mM in 0.2 mM increments. Using a final volume of 300 µL, final mixtures were obtained through the addition of 100 µL standard or protein sample, 30 µL of 10 mM DTNB and the necessary amount of working buffer. Right after DTNB addition into the mixture, an incubation time of 15 min at room temperature was set. After that time, sample absorbance at 412 nm was measured in a Varian Cary 50 spectrophotometer (Varian, California, USA; now Agilent Technologies) using a 0.3 cm quartz cuvette. Duplicates measurements were made for each NB and for the standard samples. Upon blank subtraction, a mean absorbance value was calculated for each NB, and the concentration of free cysteine was determined using the cysteine standard curve.

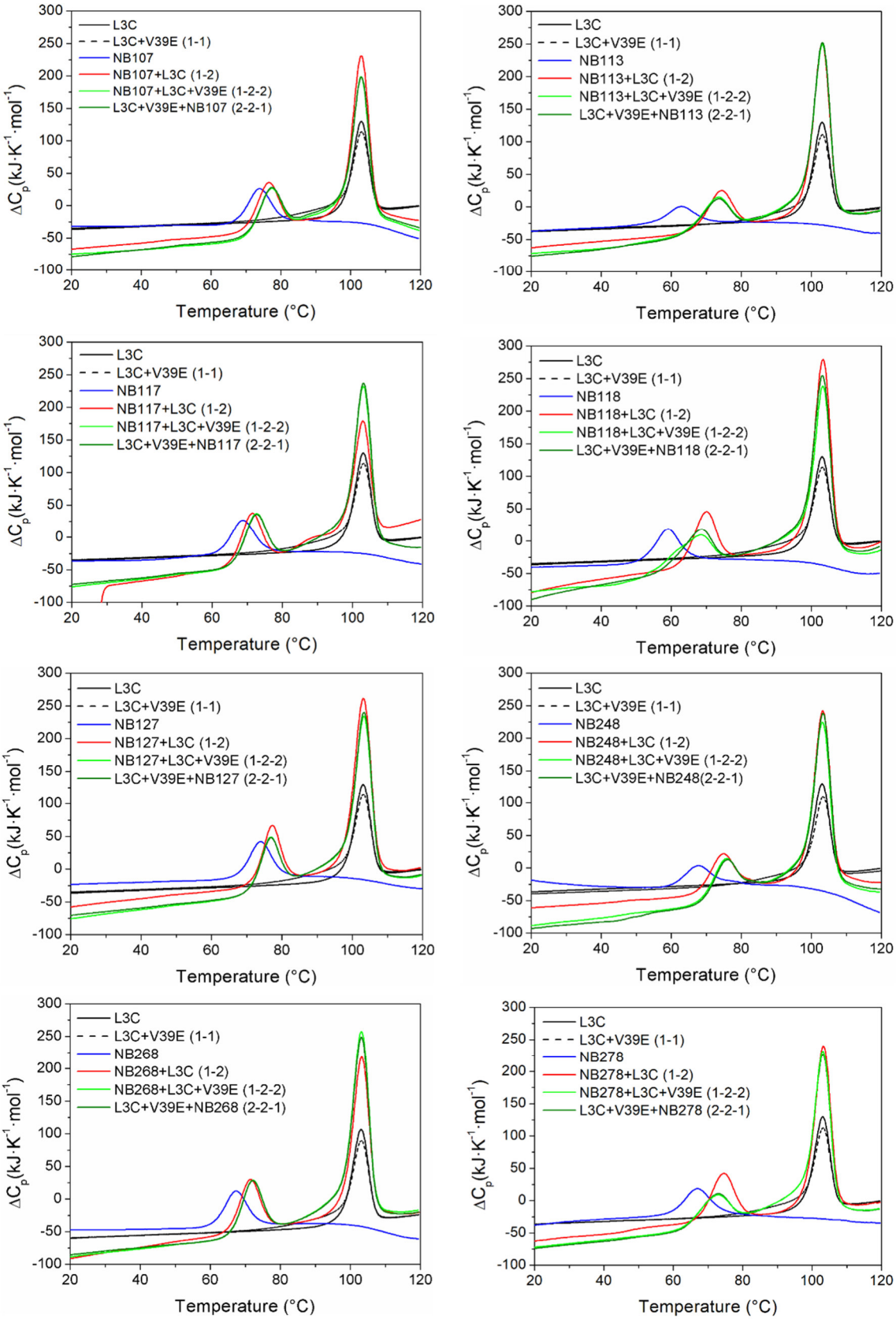

Figure S3. 1st-gen NBs differential scanning calorimetry (DSC) thermograms showing their thermal unfolding in the free form and in mixtures with L3C and the HR2-derived peptide V39E. Experiments were carried out in 50 mM phosphate buffer (pH 7.4) with a NB concentration of 20 μM and a scan rate of 90 °C/h. The molar ratio for the NB-L3C mixtures was 1-2. For ternary NB-L3C-V39E mixtures a molar ratio of 1-2-2 was used. The thermograms were normalized to the NB molar concentration.

Table S3. Biophysical properties of the 1st-and 2nd-gen NBs at pH 7.4.

NB	a.a.	Mw[a] (Da)	ε[b] ($M^{-1}\cdot cm^{-1}$)	pI[b]	R_H[c] (nm)	α-helix[c] (%)	β-sheet[c] (%)	T_m[c] (°C)	ΔH_m[c] (kJ/mol)
1st gen NBs									
107	141	15621	26150	6.39	1.9	0.7	44.8	73.5	457.4
113	119	13155	23045	8.61	1.6	0.9	44	62.1	305.0
117	146	16033	29005	5.81	1.8	1.3	43.9	68.5	442.5
118	121	13069	17085	9.14	1.7	0.6	44	57.8	392.2
127	138	15134	26025	8.59	1.8	1.1	44.4	73.8	470.6
248	128	14324	21680	7.88	1.8	1.4	43.9	66.7	335.6
268	146	16021	29005	6.64	1.9	0.8	43.2	67.1	457.1
278	123	13578	23045	8.63	1.5	1	44.6	66.8	382.2
2nd gen NBs									
147	142	15659	26025	8.59	1.9	0.6	44	67.6	293.0
184	138	15259	27515	6.70	1.8	1.1	43.9	78.7	508.3
235	142	15686	26025	8.59	1.6	0.5	44	66.8	319.3

(a) Parameter obtained using mass spectrometry analysis. NB113, NB118, NB248, and NB278 sequences are encoded in pHEN6 expression vectors and lack the hemagglutinin tag, hence their lower Mw respecting the other NBs.

(b) Theoretical parameters obtained from the NB sequence using the online software ProtParam (Expasy). Molar extinction coefficients (ε) correspond to the reduced form of the cysteine residues.

(c) Experimental data obtained in 50 mM phosphate buffer, pH 7.4. Secondary structure percentages are estimated from the far-UV CD experimental data using the K2D3 online software. T_m and ΔH_m values were obtained by fitting experimental DSC thermograms with a two-state reversible model ($Native \rightleftharpoons Unfolded$).

Table S4. Amino acid sequence of the reference HR1 used in the CoVS-HR1 proteins design, the sequences of these proteins, and the sequence of the HR2-derived peptide used in this study. Histidine tag is shown in green. Tyrosine added to V39E peptide for UV-quantification is shown in light purple.

Reference HR1 sequence	
	NVLYENQKLI ANQFNSAIGK IQDSLSSTAS ALGKLQDVVN QNAQALNTLV KQLSSNFGAI SSVLNDILSR LDKVE
CoVS-HR1 proteins[a,b]	
L3C	DVLYENQKLI ANKFNSAIKK IQDSLSSTAS ELKKLQDEVN QNAQDLNTLV KQLSSNFKRI SSELNDILSR LDKGEPAKDL RSDIDNLESK IAKFNSSLQK VLTNLAQKNQ NVEDKLKTLE SRTSSLEKQI KKIASNFQNE ILKQREYLVN KGSGNVLYEN QKLIENQFNS AIKKIQDSLS STKSALKKLK DVVNQNKQAL NTLVKQLSSN FSAISSVLND IKSRLDKVEG GGGSHHHHHH
L3B	DVLYENQKLI ANKFNSAIGK IQDSLSSTAS ELGKLQDEVN QNAQDLNTLV KQLSSNFGRI SSELNDILSR LDKGEPAKDL RSDIDNLESK IAGFNSSLQK VLTNLAQKNQ NVEDKLKGLE SRTSSLEKQI KGIASNFQNE ILKQREYLVN KGSGNVLYEN QKLIENQFNS AIGKIQDSLS STKSALGKLK DVVNQNKQAL NTLVKQLSSN FGAISSVLND IKSRLDKVEG GGGSHHHHHH
N2C	DVLYENQKLI ANKFNSAIKK IQDSLSSTAS ELKKLQDEVN KGESKKNVED KLKTLESRTS SLEKQIKKIA SNFQNEILKQ REYLVNKGSG NVLYENQKLI ENQFNSAIKK IQDSLSSTKS ALKKLKDVVN QNGGGGSHHH HHH
C2C	SELKKLQDEV NQNAQDLNTL VKQLSSNFKR ISSELNDILS RLDKGEPAKD LRSDIDNLES KIAKFNSSLQ KVLTNLAQKN QNVEDKLKKA GSDVKKLKDV VNQNKQALNT LVKQLSSNFS AISSVLNDIK SRLDKVEWGG GGSHHHHHH
HR2 derived peptide	
V39E	VDLGDISGIN ASVVNIQKEI DRLNEVAKNL NESLIDLQES GGY

(a) The residues substituted from the reference HR1 sequence are highlighted in red.

(b) Glycine residues in L3B substituted in L3C are highlighted in cyan.

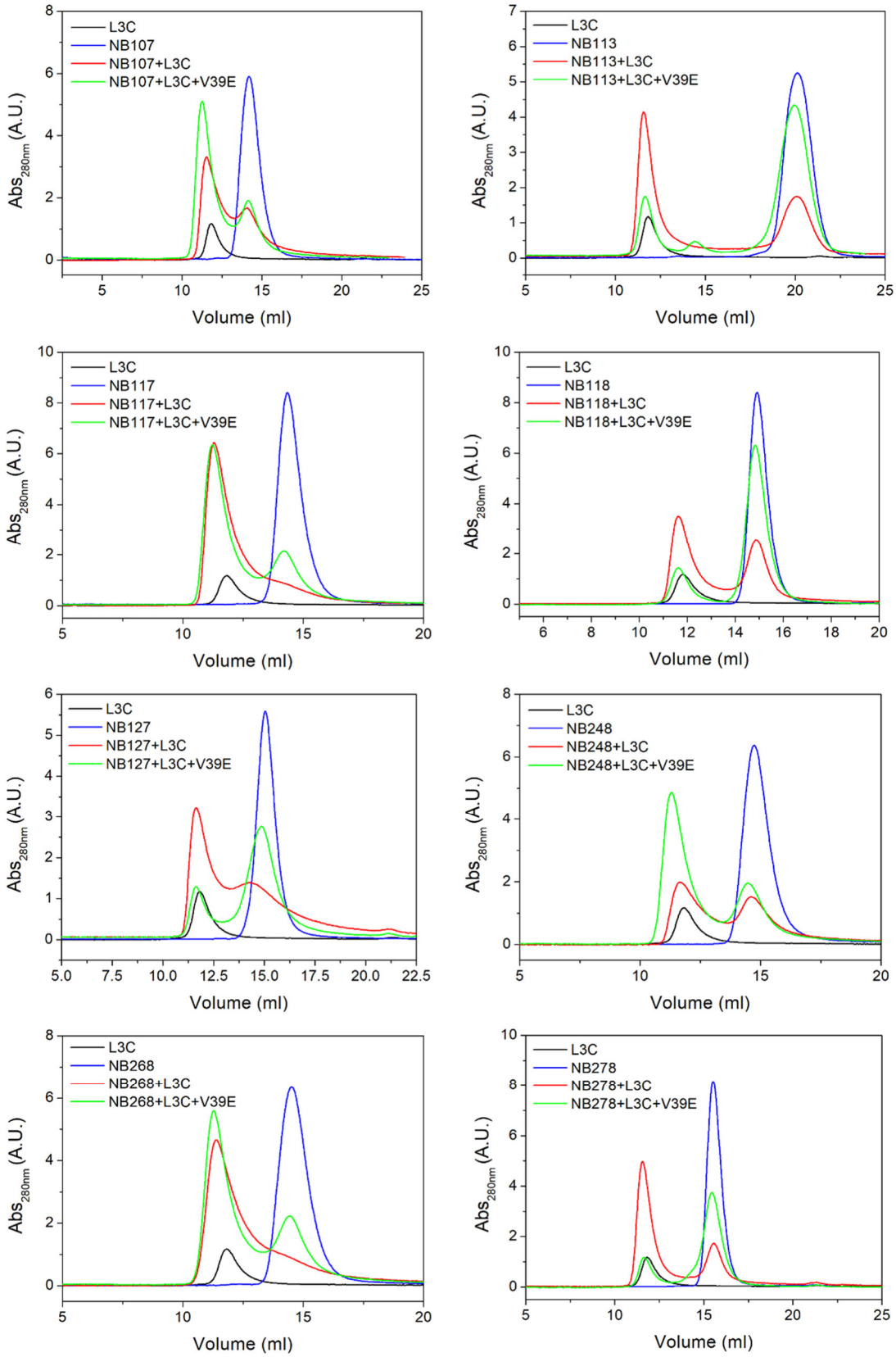

Figure S4. 1st-gen NBs size-exclusion chromatography (SEC) experiments. Chromatograms were obtained at 25 °C with an elution buffer composed of 50 mM sodium phosphate buffer (pH 7.4) and 150 mM NaCl. Elution was carried out at 1 mL/min. Molar ratios of 1:2 for the NB:L3C complexes and 1:2:2 for the NB:L3C:V39E ternary complexes were used.

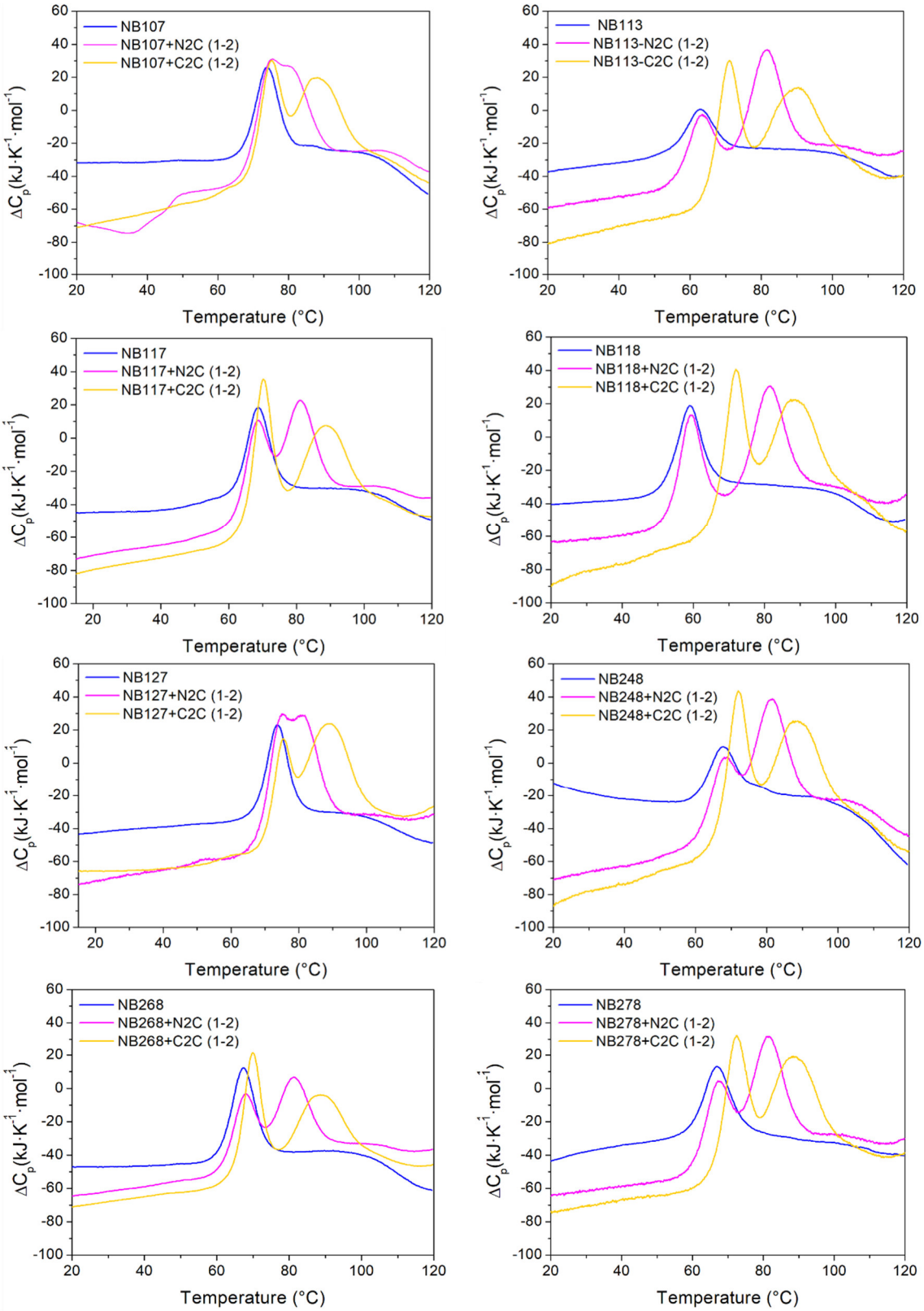

Figure S5. 1st-gen NBs DSC thermograms showing their thermal unfolding in the free form and in the mixtures with C2C and N2C proteins. Experiments were carried out in 50 mM phosphate buffer (pH 7.4) with a NB concentration of 20 μM and a scan rate of 90 °C/h. For NB:N2C/C2C mixes, a molar ratio 1:2 was used. The thermograms were normalized to the NB molar concentration.

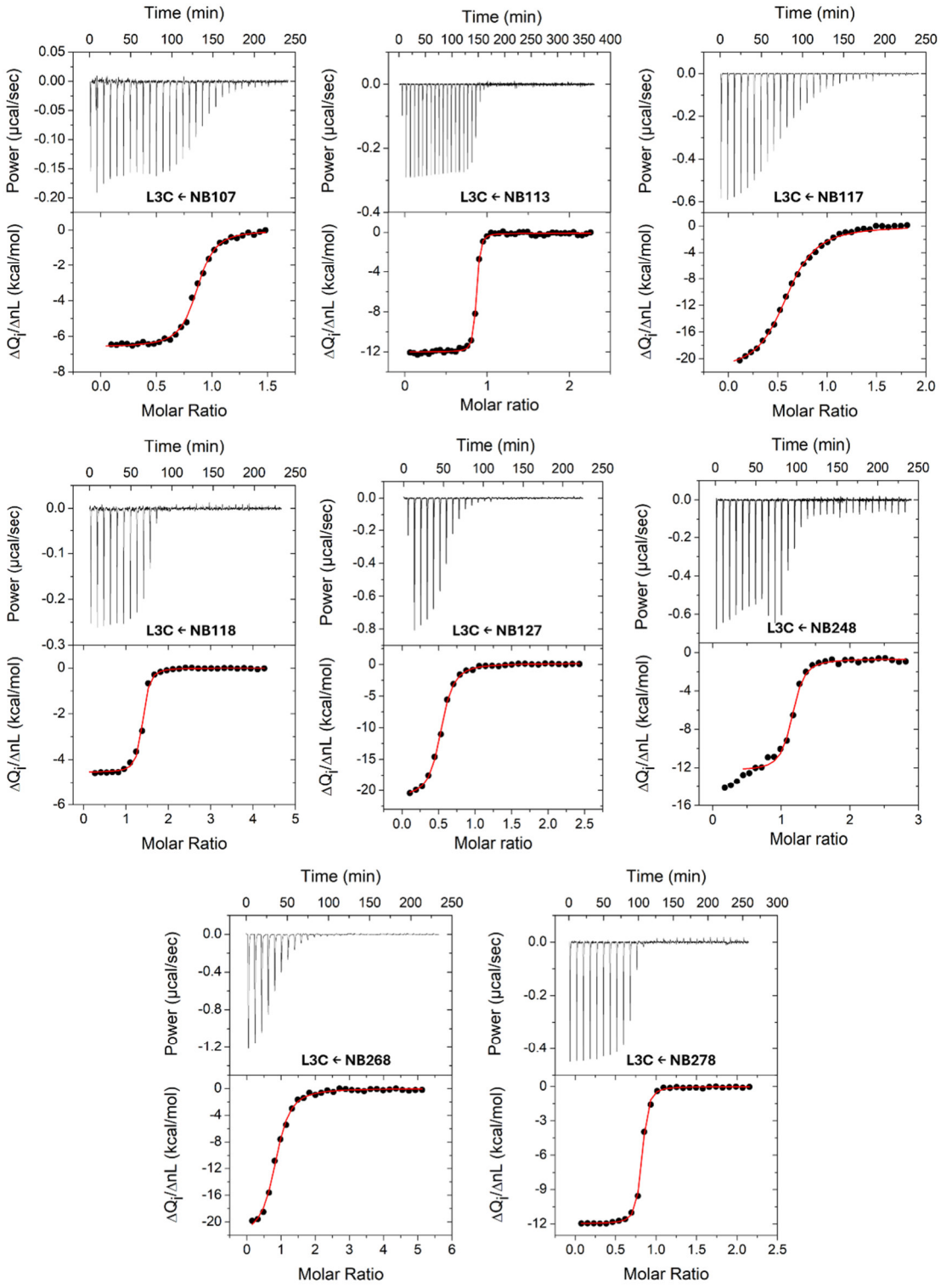

Figure S6. 1st-gen NBs isothermal titration calorimetry (ITC) experiments. All measures were carried out at 25 °C in 50 mM phosphate buffer (pH 7.4). The upper panel represents the experimental thermogram corrected from baseline with negative heats of binding. The red lines correspond to the best fits using a model of n identical and independent sites. Due to its higher binding affinity, for NB113 titration a total of 60 injections of 5 µl were programmed to achieve enough data points in the slope region.

Table S5. Thermodynamic parameters of the interaction NB–L3C measured by ITC. Data obtained at 25 °C, unless stated otherwise.

NB	n	K_b ($\cdot 10^{-6} \cdot M^{-1}$)	K_d (μM)	ΔG (kJ/mol)	ΔH (kJ/mol)	T·ΔS (kJ/mol)
1st-gen NBs						
NB107	0.84	9.5 ± 2.3	0.16 ± 0.025	−39.8 ± 0.3	−28.9 ± 1.0	+10.9 ± 1.6
NB113	0.85	211 ± 4	0.0047 ± 0.0009	−47.5 ± 0.5	−50 ± 0.4	-2.5 ± 0.9
NB117	0.6	1.93 ± 0.18	0.52 ± 0.05	−35.87 ± 0.23	−97.6 ± 2.2	−61.7 ± 2.4
NB118	1.3	33 ± 12	0.030 ± 0.011	−42.9 ± 0.9	−18.1 ± 0.4	+24.8 ± 1.3
NB127	0.5	6.9 ± 0.9	0.144 ± 0.018	−39.1 ± 0.3	− 89.1 ± 1.6	−50.1 ± 1.9
NB248	1.1	16 ± 6.0	0.063 ± 0.024	−41.1 ± 1.0	−48.6 ± 1.9	−8 ± 3
NB268	0.8	2.1 ± 0.3	0.47 ± 0.07	−36.1 ± 0.4	−92 ± 3	−56 ± 3
NB278	0.8	81 ± 18	0.012 ± 0.003	−45.1± 0.5	−48.7 ± 0.6	−3.5 ± 1.2
2nd-gen NBs						
NB147(*)	1(f)	0.03 ± 0.03	32 ± 30	−26.6 ± 2.2	−76 ± 60	−49 ± 60
NB184(*)	0.9	0.65 ± 0.12	1.5 ± 0.3	−34.5 ± 0.5	−47 ± 3	−13 ± 3
NB184	1.3	1.1 ± 0.3	0.9 ± 0.3	−34.6 ± 0.8	−15.1 ± 1.0	+19.5 ± 1.7
NB235(*)	1(f)	0.20 ± 0.14	5 ± 3	−31.5 ± 1.7	−22 ± 7	+9 ± 9
Cooperative Effect						
113 (+2:1 184)	0.82	243 + 60	0.0041 ± 0.0010	-47.9 ± 0.6	-51.8 ± 0.5	-4.0 ± 1.1
118 (+2:1 184)	0.9	45 ± 14	0.022 ± 0.007	−43.7 ± 0.7	−20.6 ± 0.3	+23.2 ± 1.1
278 (+2:1 184)	0.82	110 ± 25	0.0091 ± 0.0020	−45.9 ± 0.6	−46.2 ± 0.5	−0.3 ± 1.1
184 (+1.5:1 113) (*)	0.80	1.2 ± 0.4	0.81 ± 0.23	-36.2 ± 0.7	-40 ± 3	-4 ± 3
184 (+1.5:1 118) (*)	0.92	1.04 ± 0.13	0.96 ± 0.12	−35.7 ± 0.3	−41.5 ± 1.4	−5.0 ± 1.5
184 (+1.5:1 278) (*)	0.91	1.40 ± 0.15	0.71 ± 0.08	−36.5 ± 0.3	−39.7 ± 0.9	−3.2 ± 1.2

(f) Parameter fixed for an appropriate fitting to the n-independent binding sites model.
(*) Experiments carried out at 37 °C.

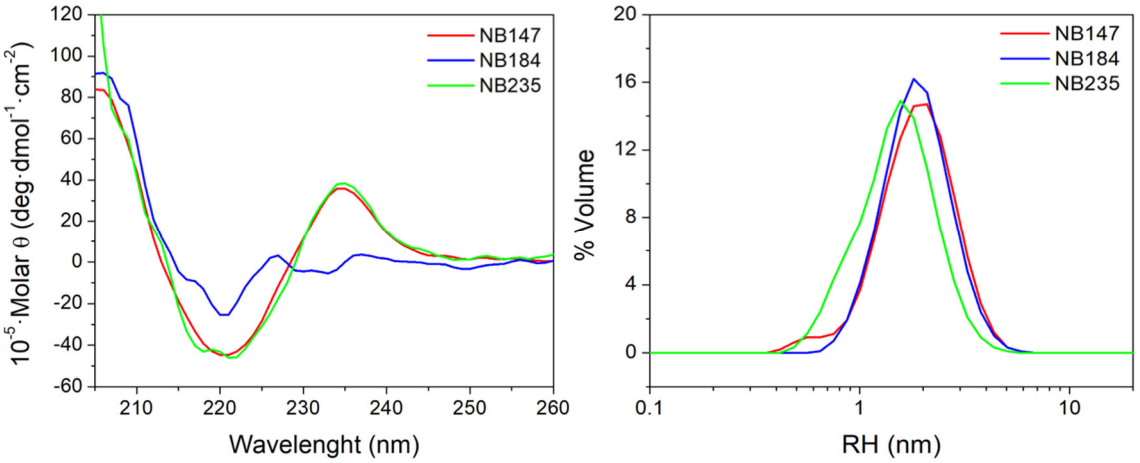

Figure S7. 2nd-gen NBs far-UV CD spectra (left) and Rh distributions obtained by DLS (right). Experiments were carried out at 25 °C in 50 Mm phosphate buffer (pH 7.4) and a protein concentration of 25 μM. All NBs showed a CD spectrum typical of β-sheet rich proteins and R_h between 1.6 and 1.9 nm, consistent with a monomeric state of the molecules.

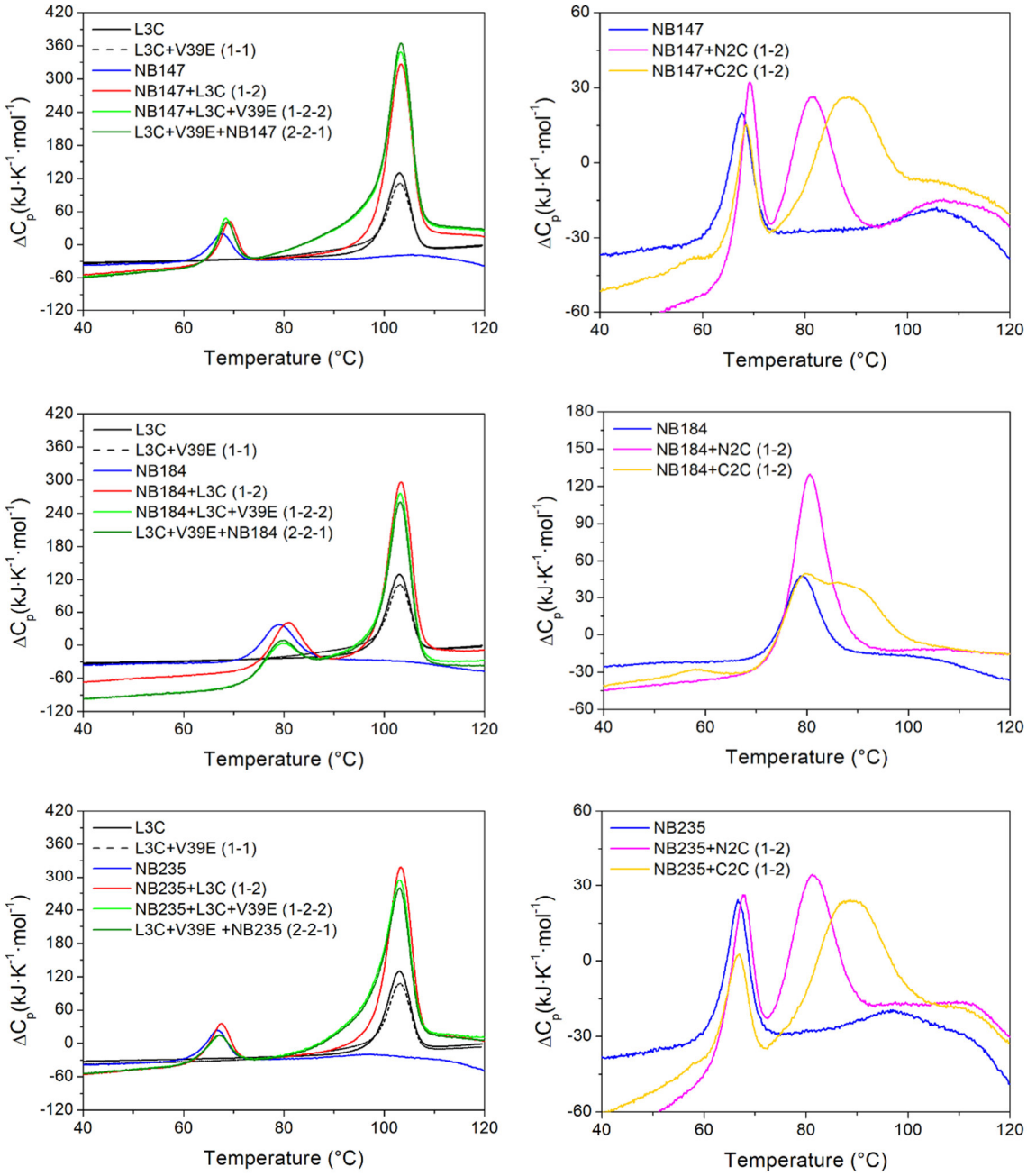

Figure S8. 2nd-gen NBs DSC thermograms showing their thermal unfolding in the free form and in the mixtures with L3C, V39E, N2C, and C2C proteins. Experiments were carried out in 50 mM phosphate buffer (pH 7.4) with a NB concentration of 20 μM and a scan rate of 90 °C/h. For NB:(L3C, N2C or C2C) mixtures, a molar ratio 1:2 was used. For the ternary complexes NB:L3C:V39E, the peptide was added to meet a molar ratio 1:2:2. The thermograms were normalized to the NB molar concentration.

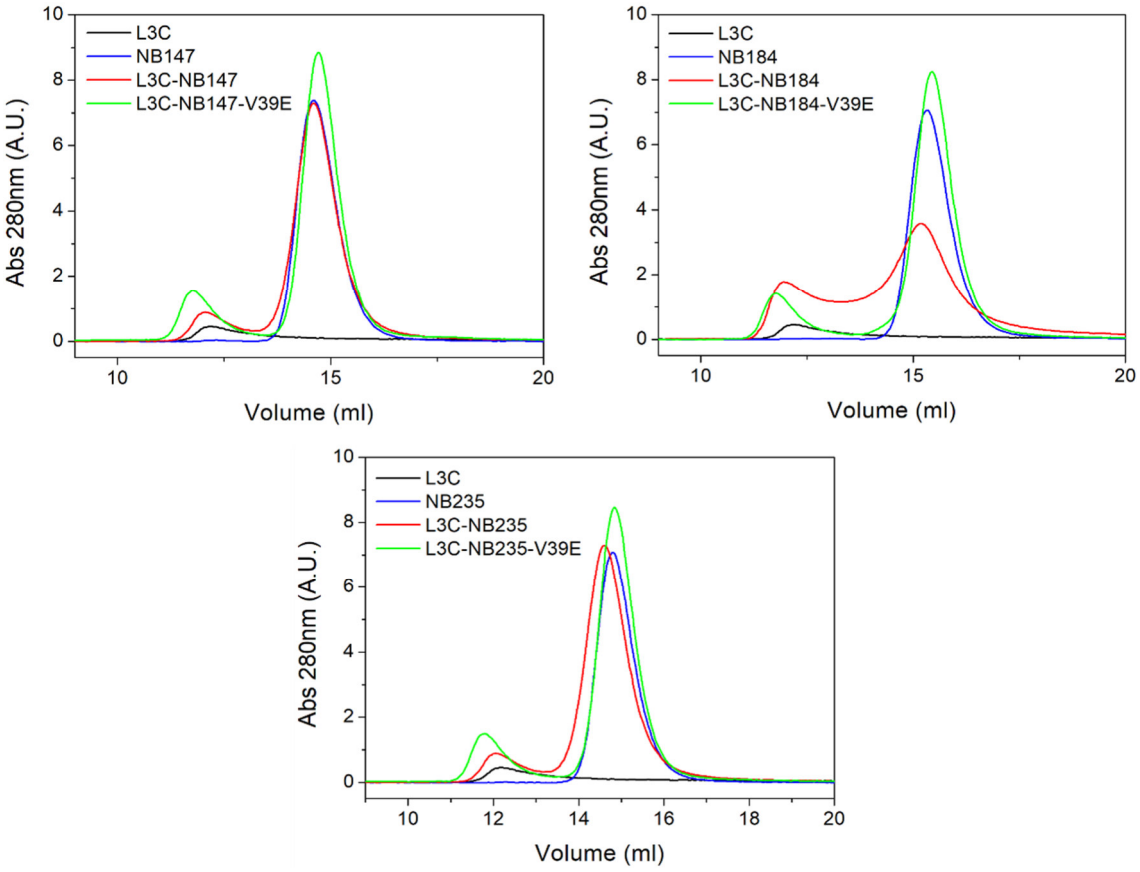

Figure S9. 2nd-gen NBs SEC experiments. Chromatograms were obtained at 25 °C with an elution buffer composed of 50 mM sodium phosphate buffer (pH 7.4) containing 150 mM NaCl. Elution was carried out at 1 mL/min. Molar ratios of 1:2 for the NB:L3C complexes and 1:2:2 for the NB:L3C:V39E ternary complexes were used.

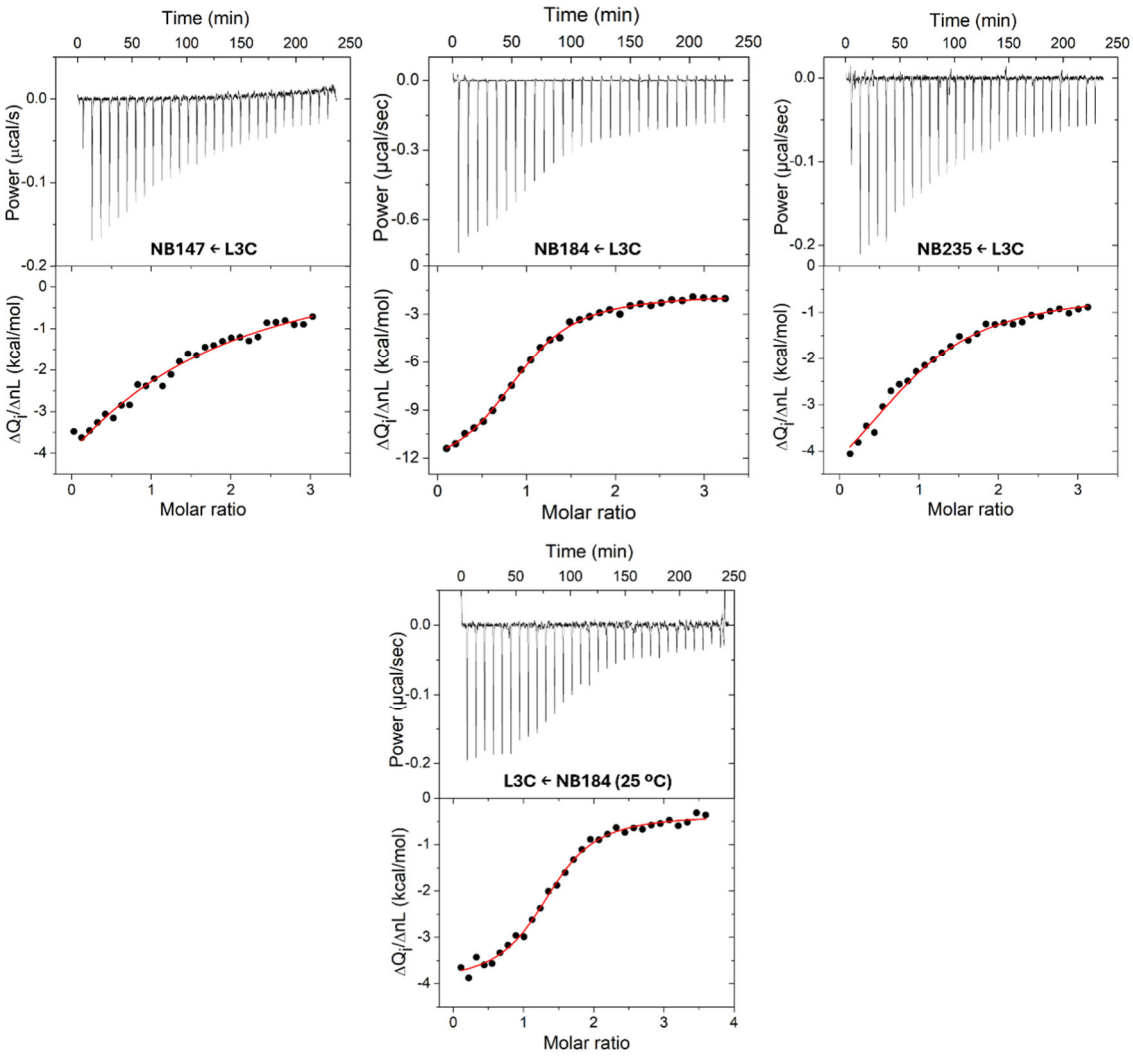

Figure S10. 2nd-gen NBs ITC experiments. All measures were carried out at 37 °C in 50 mM phosphate buffer (pH 7.4). Titration of L3C with NB184 at 25 °C is also included. The upper panel represents the experimental thermogram corrected from baseline with negative heats of binding. The red lines correspond to the best fits using a model of n identical and independent sites.

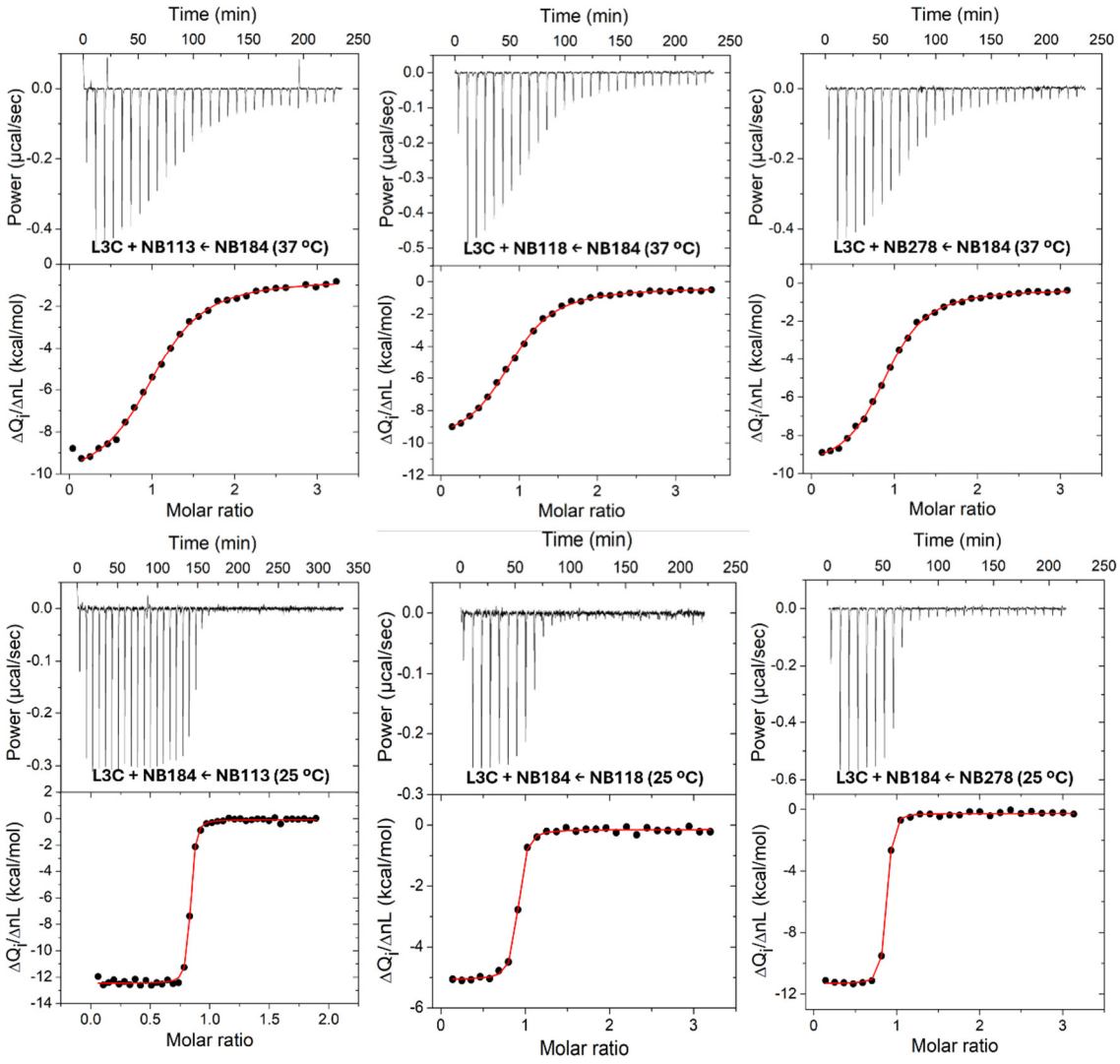

Figure S11. Combined ITC experiments between NB184 and the 1st-gen NBs: NB113, NB118, and NB278. All experiments where NB184 was used as titrant were carried out at 37 °C, while the complementary titrations with the 1st gen NBs were conducted at 25 °C, as indicated in the figure. The upper panels represent the experimental thermogram corrected from baseline with negative heats of binding. The red lines correspond to the best fits using a model of n identical and independent sites.

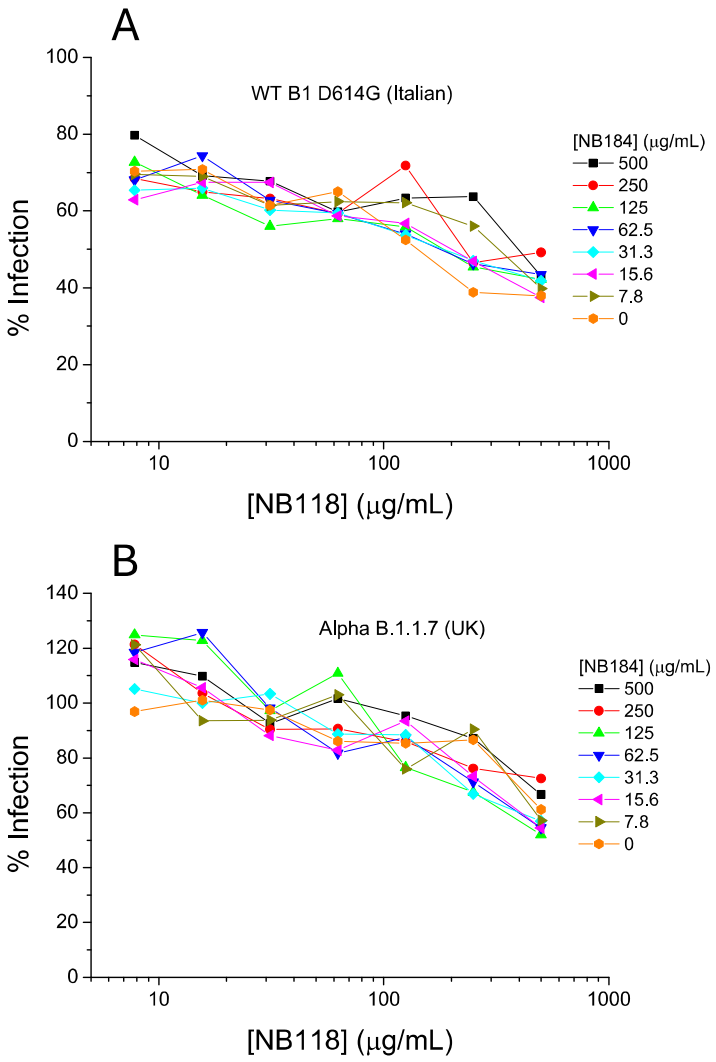

Figure S12. Combination neutralization assays with NB118 and NB184. Vero 76 cells were infected with SARS-CoV-2 WT B.1 with D614G isolate (A) or the BA.1.1.7 (UK) isolate (B) in the presence of variable concentrations of NB118 and NB184 as indicated in μg/mL. The percentage of infection was calculated as the percentage of infected cells in presence of the NBs divided by the percentage of infected cells in control wells without NBs.

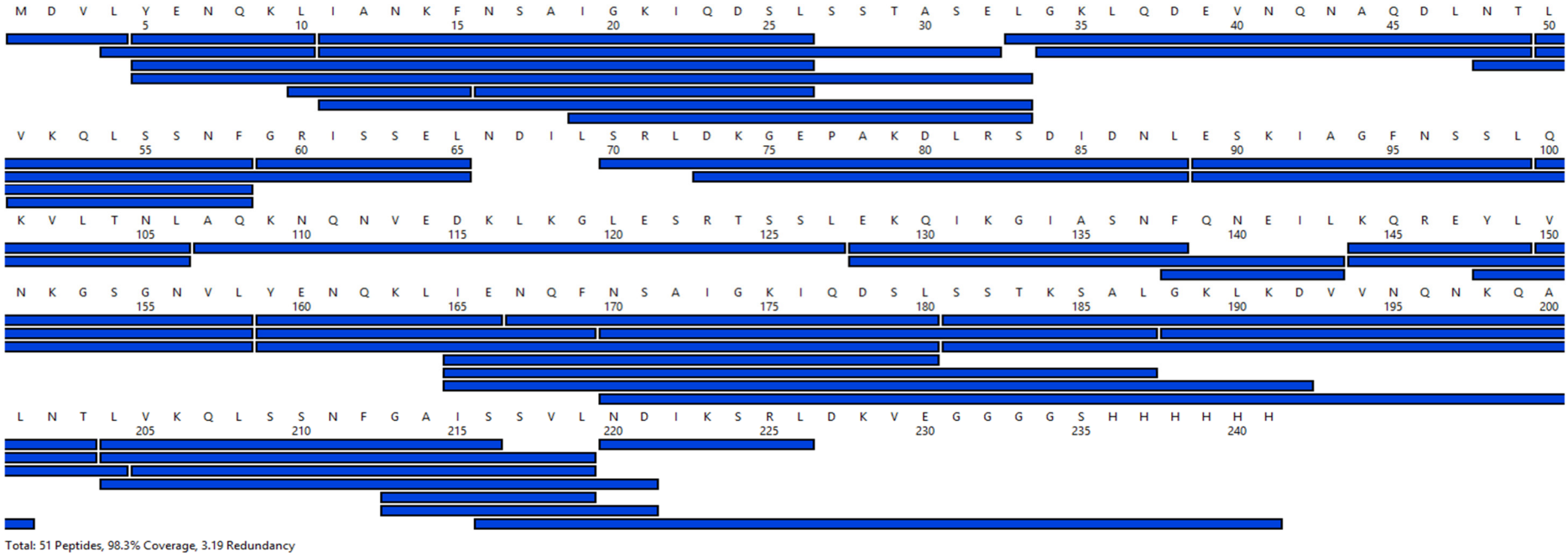

Figure S13. L3B coverage map obtained after digestion on an in-line pepsin column, followed by separation and analysis of the resulting peptic fragments using ultraperformance liquid chromatography–mass spectrometry (UPLC–MS). Before digestion the protein was incubated for 4 min at 0 °C in quenching buffer consisting of 7 M guanidine hydrochloride (Gnd-HCl), 0.8% formic acid, adjusted to pH 2.21.

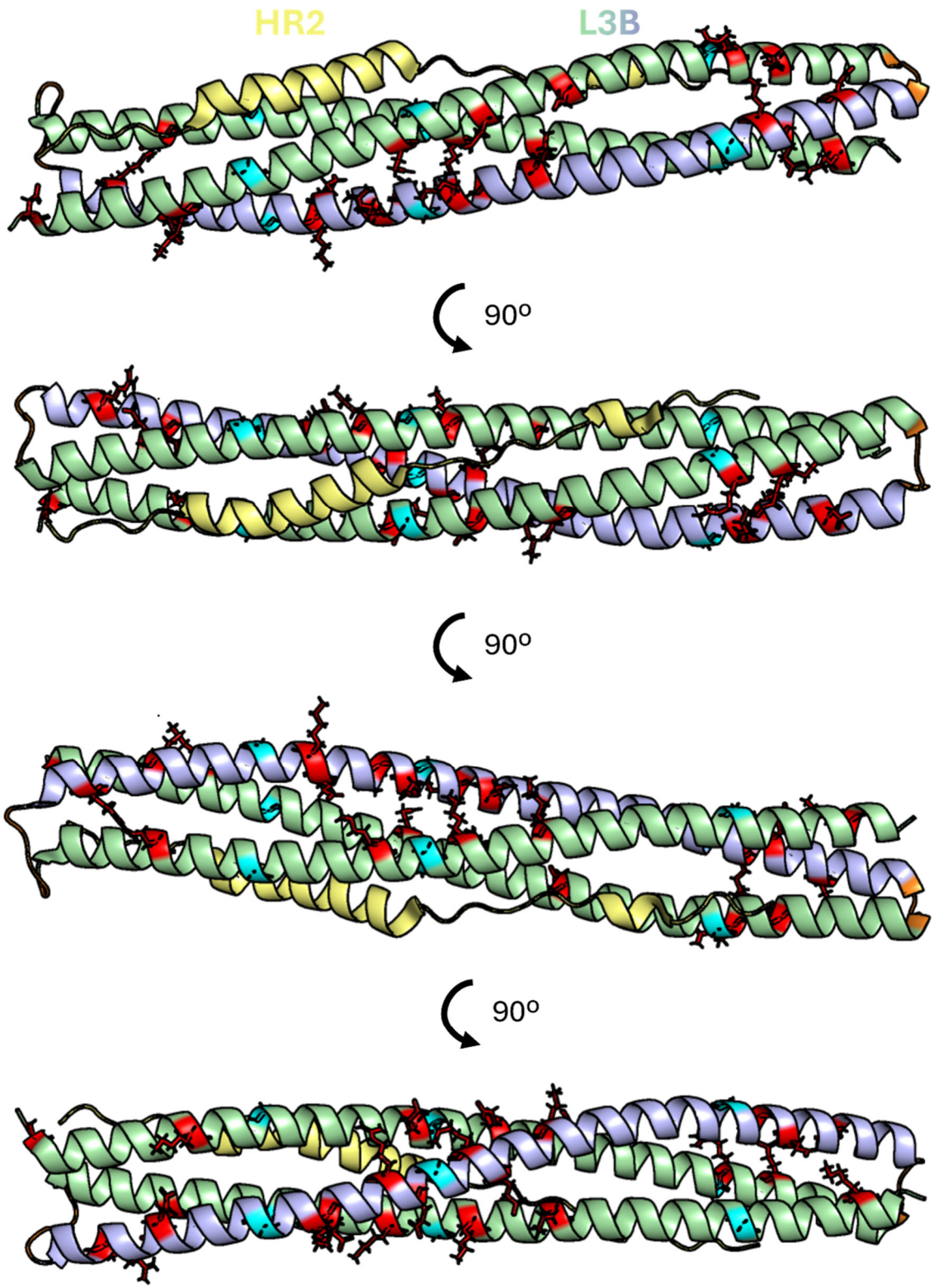

Figure S14. Mutations of the CoVS-HR1 proteins plotted on the L3B–HR2 complex. Crystallographic structure of the CoVS-HR1-L3B protein in complex with the HR2-derived peptide V39E (PDB ID: 7ZR2) with the mutations respecting the original HR1 sequence represented as red sticks. Additionally, glycine residues that are replaced in L3C (by mainly lysine residues) are represented as cyan sticks (see Table S4). The two parallel helices forming the HR2-binding groove are colored in light green while the antiparallel helix is colored in light blue.

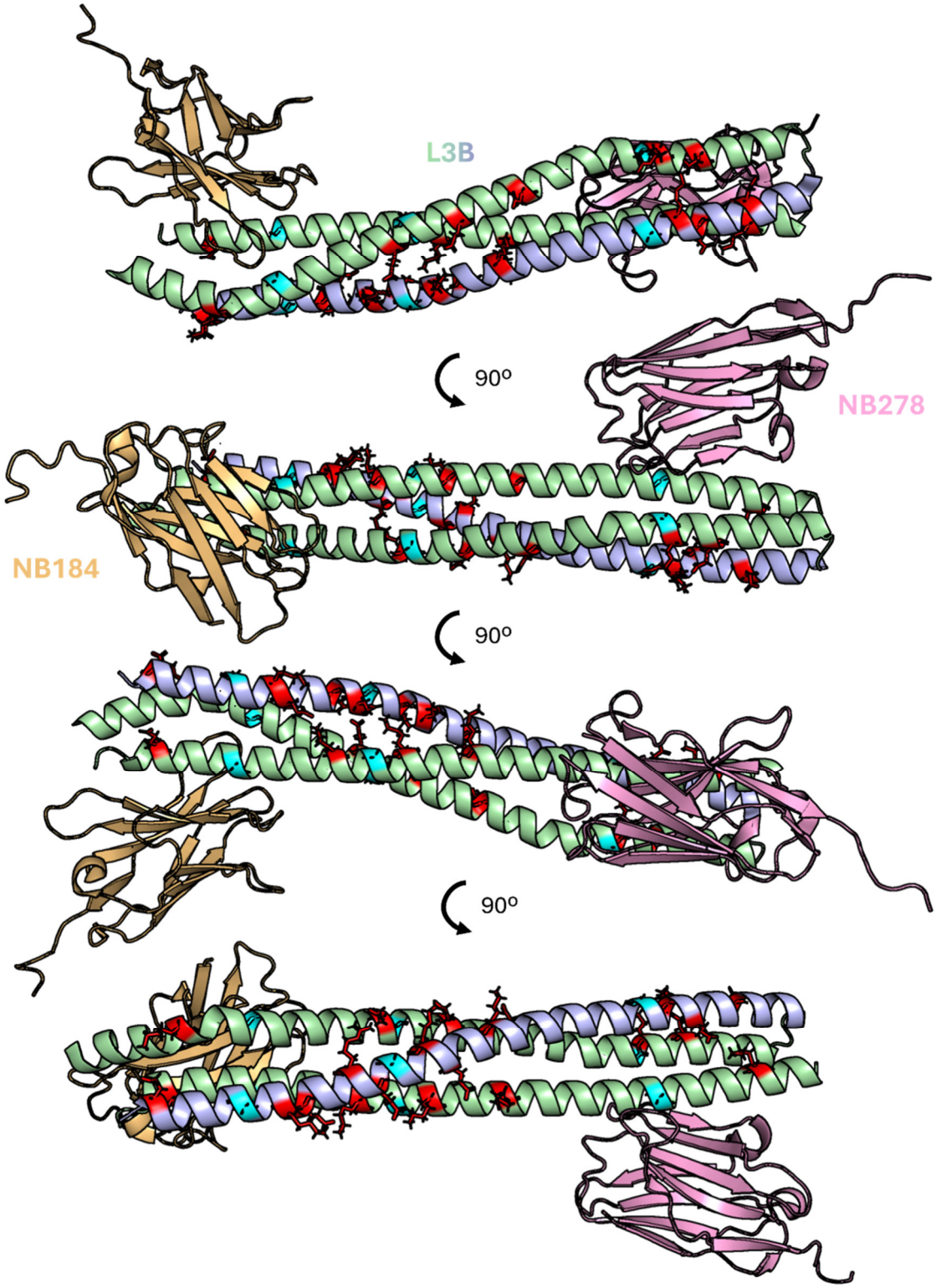

Figure S15. Mutations of the CoVS-HR1 proteins plotted on the L3B–NB184–NB278 complex. Crystallographic structure of the CoVS-HR1-L3B protein in complex with NB184 and NB278 (PDB ID: 9RN6) with the mutations respecting the original HR1 sequence represented as red sticks. Additionally, glycine residues that are replaced in L3C (by mainly lysine residues) are represented as cyan sticks (see Table S4). The two parallel helices forming the HR2-binding groove are colored in light green while the antiparallel helix is colored in light blue.

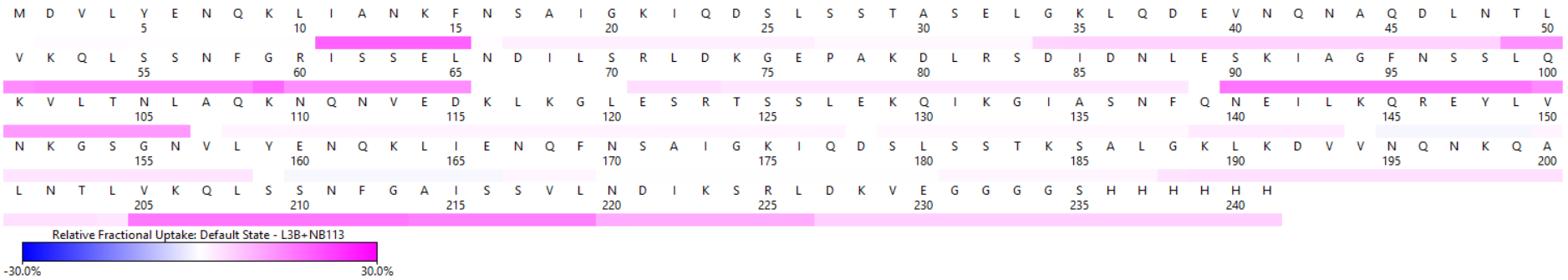

L3B–NB113

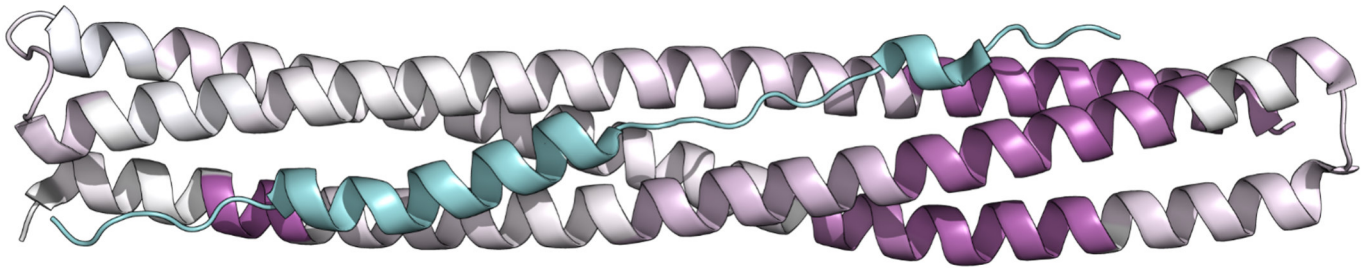

Figure S16-A. HDX heat maps showing the difference in relative uptake between the default state (i.e., L3B alone) and the protein incubated with NB113. Results from the heat map are plotted onto the crystallographic structure of L3B in complex with the HR2-derived peptide V39E (PDB ID: 7ZR2). Areas colored in magenta show lower exchange in complex with the NB compared with the free state, while white areas do not undergo any change in HDX.

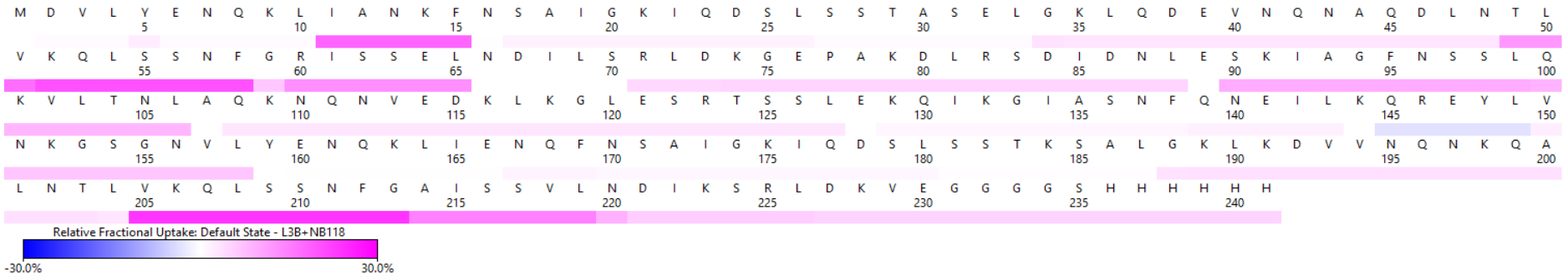

L3B–NB118

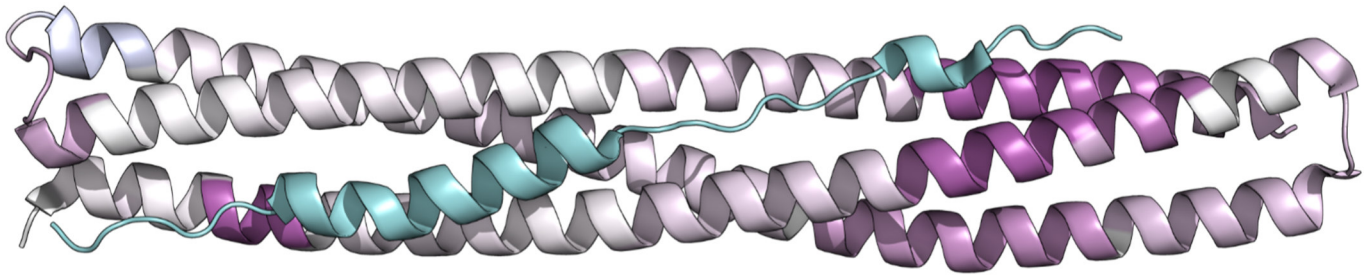

Figure S16-B. HDX heat maps showing the difference in relative uptake between the default state (i.e., L3B alone) and the protein incubated with NB118. Results from the heat map are plotted onto the crystallographic structure of L3B in complex with the HR2-derived peptide V39E (PDB ID: 7ZR2). Color gradient is the same as in Fig 16-A.

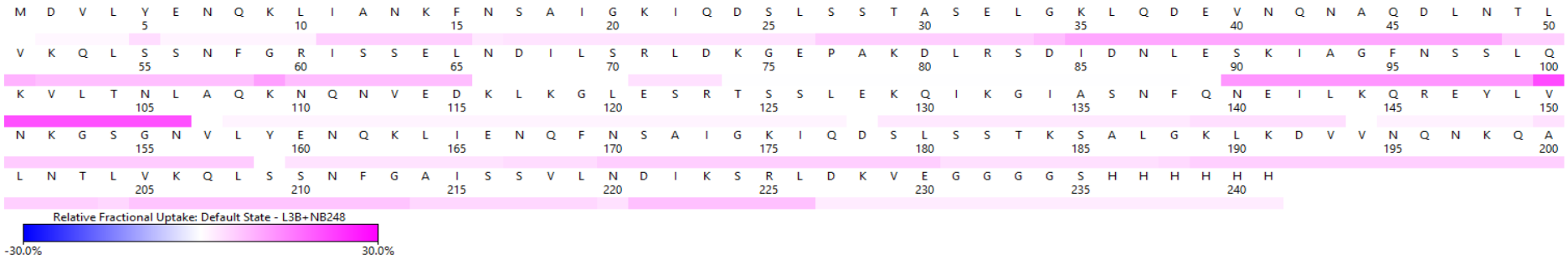

L3B–NB248

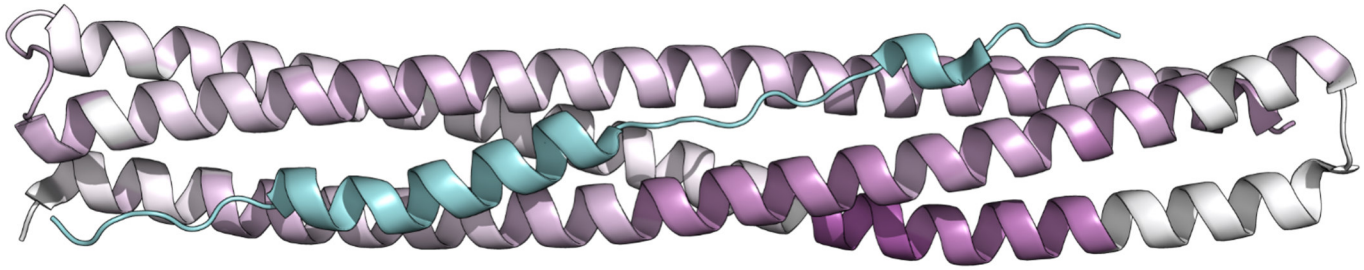

Figure S16-C. HDX heat maps showing the difference in relative uptake between the default state (i.e., L3B alone) and the protein incubated with NB248. Results from the heat map are plotted onto the crystallographic structure of L3B in complex with the HR2-derived peptide V39E (PDB ID: 7ZR2). Color gradient is the same as in Fig 16-A.

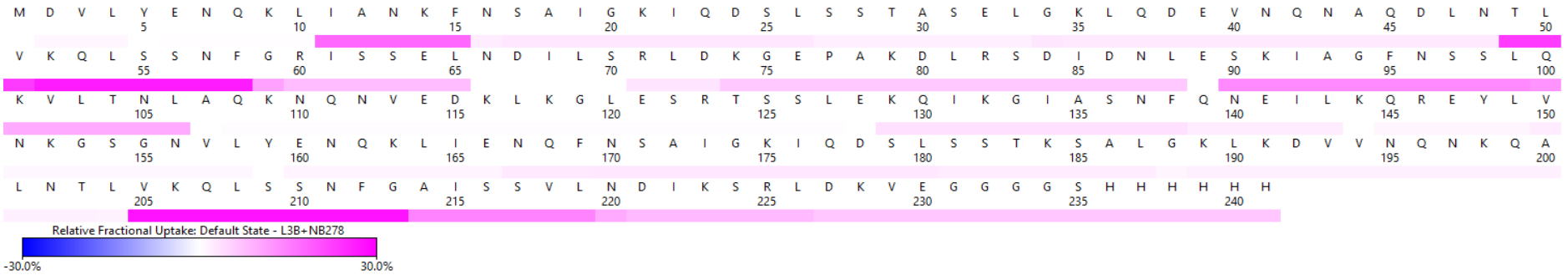

L3B–NB278

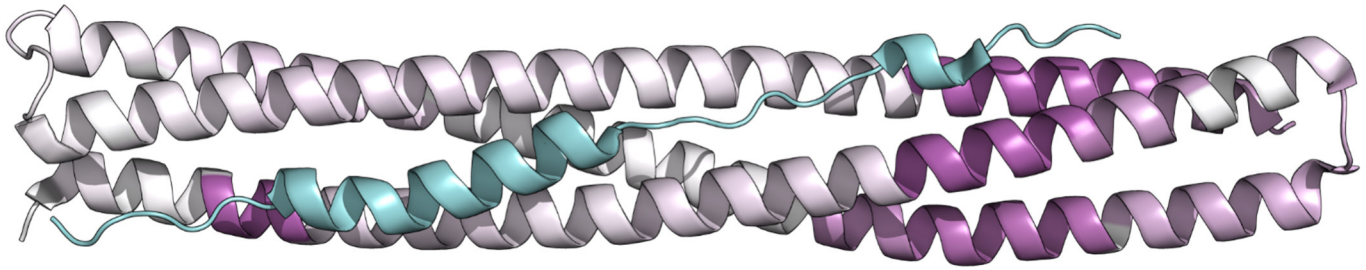

Figure S16-D. HDX heat maps showing the difference in relative uptake between the default state (i.e., L3B alone) and the protein incubated with NB278. Results from the heat map are plotted onto the crystallographic structure of L3B in complex with the HR2-derived peptide V39E (PDB ID: 7ZR2). Color gradient is the same as in Fig 16-A.

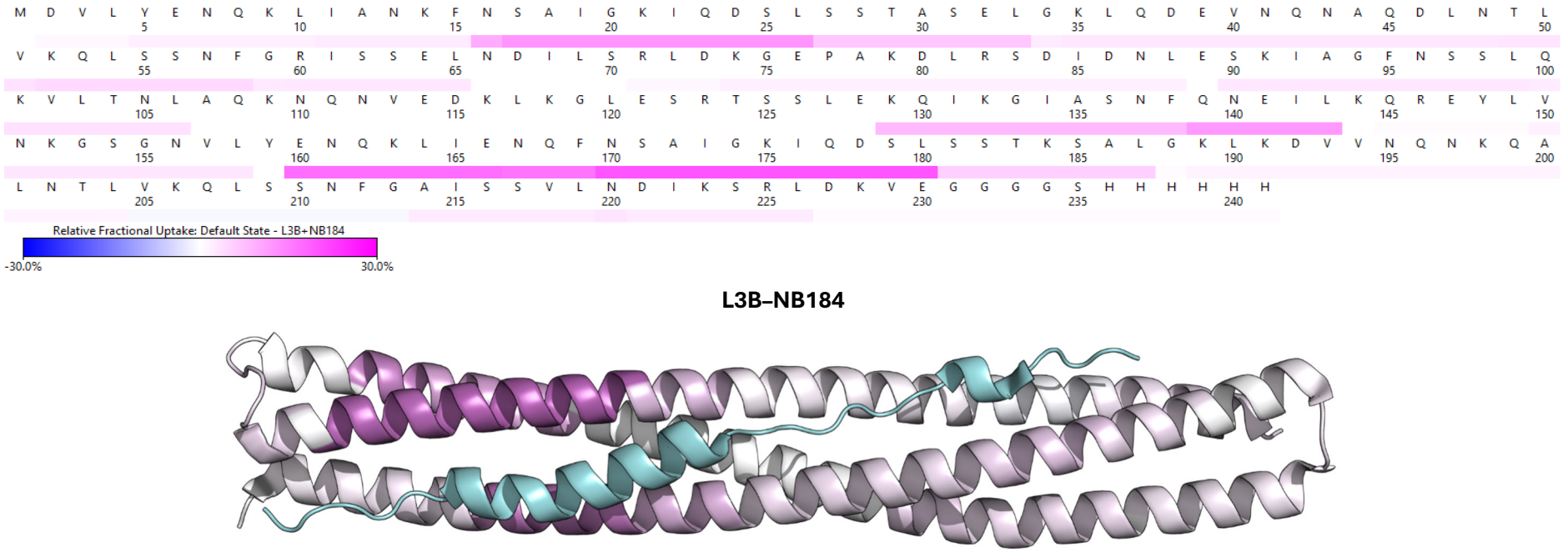

Figure S16-E. HDX heat maps showing the difference in relative uptake between the default state (i.e., L3B alone) and the protein incubated with NB184. Results from the heat map are plotted onto the crystallographic structure of L3B in complex with the HR2-derived peptide V39E (PDB ID: 7ZR2). Color gradient is the same as in Fig 16-A.

Table S6. Quantitative analysis of the contact surfaces between L3B and nanobody NB278. The table presents the total intermolecular surface area (in Å^2) calculated from both the L3B and nanobody sides of the interface, along with the relative contributions of polar and apolar residues involved in each interaction surface.

L3B			**NB278**		
Total Area of Interaction (Å^2)	516		Total Area of Interaction (Å^2)	496.36	
Hydrophobic Area of Interaction (Å^2)	341.18		Hydrophobic Area of Interaction (Å^2)	324.9	
% of contact surface that is hydrophobic	66.1		% of contact surface that is hydrophobic	65.5	
Residues from L3B interacting with NB278			Residues from NB278 interacting with L3B		
Residue	Residue Number	Area of interaction	Residue	Residue Number	Area of interaction
LEU	54	11.54	SER	30	0.19
SER	55	19.59	ASN	31	30.22
PHE	58	36.87	ASN	32	12.47
GLY	59	9.53	ALA	33	29.08
SER	62	17.64	TYR	37	7.2
LEU	65	0.19	LEU	47	40.33
LEU	69	13.57	ASN	50	25.9
THR	203	13.55	ILE	51	0.17
LYS	206	24.07	ILE	52	48.93
GLN	207	38.98	THR	53	30.24
SER	209	18.95	PHE	54	57.5
SER	210	44.46	ASN	56	20.22
ASN	211	48.35	TYR	58	59.51
GLY	213	12.61	THR	60	13.95
ALA	214	41.58	ASP	61	25.95
ILE	215	14.67	TYR	98	57.92
SER	217	30.09	GLY	99	10.95
VAL	218	44.17	ASP	100	25.63
ASP	221	35.43			
ILE	222	15.11			
ARG	225	25.05			

Table S7. Quantitative analysis of the contact surfaces between L3B and nanobody NB184. The table presents the total intermolecular surface area (in Å^2) calculated from both the L3B and nanobody sides of the interface, along with the relative contributions of polar and apolar residues involved in each interaction surface.

L3B			**NB184**		
Total Area of Interaction (Å^2)		525.45	Total Area of Interaction (Å^2)		527.46
Hydrophobic Area of Interaction (Å^2)		362.09	Hydrophobic Area of Interaction (Å^2)		360.65
% of contact surface that is hydrophobic		68.9	% of contact surface that is hydrophobic		68.4
Residues from L3B interacting with NB184			Residues from NB184 interacting with L3B		
Residue	Residue Number	Area of interaction	Residue	Residue Number	Area of interaction
LYS	9	19.53	ASP	33	10.91
ALA	12	22.76	PHE	37	24.55
ASN	13	13.6	GLU	44	1.12
PHE	15	0.08	ARG	45	19.5
ASN	16	30.46	GLU	46	5.99
ILE	19	28.29	PHE	47	39.37
GLY	20	11.8	ASP	50	23.46
GLN	23	14.04	ILE	51	3.6
PHE	138	1.22	ARG	52	28.69
LYS	163	2.33	SER	55	0.6
LEU	164	45.01	SER	57	34.4
ILE	165	22.35	THR	58	8.13
ASN	167	40.04	TYR	59	60.53
GLN	168	61.15	ALA	61	8.8
PHE	169	32.55	ASP	62	8.22
ASN	170	19.77	ARG	99	33.87
SER	171	36.08	PRO	101	6.41
ALA	172	30.06	GLY	102	29.45
ILE	173	1.09	GLY	103	19.05
GLY	174	3.08	ILE	104	77.62
LYS	175	74.09	LEU	105	56.02
ASP	178	16.07	TYR	106	22.54
			TRP	109	4.63

Table S8. Interaction analysis between L3B and NB278.

Hydrophobic interactions (cutoff distance: 5 Å)			
Molecule	Residue	Number of contacts [(a)]	Interaction Strength [(b)]
NB278	ASN 31	1	0.649
	ALA 33	2	1.536
	LEU 47	4	3.431
	ILE 52	8	7.782
	THR 53	1	0.627
	PHE 54	6	4.749
	ASN 56	1	0.716
	TYR 58	10	6.086
	ASP 61	1	0.578
	TYR 98	3	2.548

Pi-Pi interactions (cutoff distance: 5 Å)			
Chain	Residue	Number of contacts [(c)]	Interaction Strength [(d)]
B (NB278)	PHE 54	4	2.222

Hydrogen bonds			
Group from L3B	Group from NB278	Distance (Å)	Energy [(e)]
OD1 ASN 211	N THR 53	2.15	22.35
OD2 ASP 221	OH TYR 58	2.16	7.9

Ionic Interactions			
Group from L3B	Group from NB278	Number of Interactions	Interaction Strength
LYS 206	ASP 100	1	0.482
ARG 225	ASP 61	1	1

(a) Number of contacts involving different carbon atoms (methyl, methylene, methine or aromatic).
(b) Estimated by YASARA software using a knowledge-based potential as described in the software manual. An interaction strength > 5 indicates a strong interaction.
(c) Contacts involving atoms in planar rings.
(d) Interaction strengths range from 0 to 1.
(e) Interaction energy calculated using a simple potential as described in the software manual. Energy ranges from 6.25 (minimun) to 25 kJ/mol (optimum).

Table S9. Interaction analysis between L3B and NB184.

Hydrophobic interactions (cutoff distance: 5 Å)			
Molecule	Residue	Number of contacts [(a)]	Interaction Strength [(b)]
NB184	PHE 37	4	2.614
	ARG 45	2	1.22
	PHE 47	7	4.447
	ASP 50	1	0.346
	ARG 52	4	2.923
	SER 57	2	1.085
	TYR 59	4	2.431
	GLY 102	2	1.349
	GLY 103	1	0.868
	ILE 104	12	7.607
	LEU 105	9	7.379
	TYR 106	1	0.963

Pi-Pi interactions (cutoff distance: 5 Å)			
Chain	Residue	Number of contacts [(c)]	Interaction Strength [(d)]
None			

Hydrogen bonds			
Group from L3B	Group from NB184	Distance (Å)	Energy [(e)]
OE1 GLN 23	N GLY 102	2.27	14.48
O GLN 168	NH1 ARG 99	2.11	10.35
OE1 GLN 168	N TYR 106	2.27	16.48

Ionic Interactions			
Group from L3B	Group from NB184	Number of Interactions	Interaction Strength
LYS 163	ASP 62	1	0.581
LYS 175	ASP 50	1	0.606

(a) Number of contacts involving different carbon atoms (methyl, methylene, methine or aromatic).
(b) Estimated by YASARA software using a knowledge-based potential as described in the software manual. An interaction strength > 5 indicates a strong interaction.
(c) Contacts involving atoms in planar rings.
(d) Interaction strengths range from 0 to 1.
(e) Interaction energy calculated using a simple potential as described in the software manual. Energy ranges from 6.25 (minimun) to 25 kJ/mol (optimum).

Supplementary bibliography.

[1] E. Pardon, T. Laeremans, S. Triest, S.G.F. Rasmussen, A. Wohlkönig, A. Ruf, S. Muyldermans, W.G.J. Hol, B.K. Kobilka, J. Steyaert, A general protocol for the generation of Nanobodies for structural biology, Nat Protoc 9 (2014) 674–693. https://doi.org/10.1038/nprot.2014.039.

[2] M. Cano-Muñoz, D. Polo-Megías, A. Cámara-Artigas, J.A. Gavira, M.J. López-Rodríguez, G. Laumond, S. Schmidt, J. Demiselle, S. Bahram, C. Moog, F. Conejero-Lara, Novel chimeric proteins mimicking SARS-CoV-2 spike epitopes with broad inhibitory activity, Int J Biol Macromol 222 (2022) 2467–2478. https://doi.org/10.1016/j.ijbiomac.2022.10.031.

[3] P.A. Karplus, K. Diederichs, Linking Crystallographic Model and Data Quality, Science (1979) 336 (2012) 1030–1033. https://doi.org/10.1126/science.1218231.

[4] A. Parody-Morreale, C. Baron, Visualization of protein denaturation by chemical modification of sulfhydryl groups: Undergraduate macromolecular chemistry experiment, J Chem Educ 63 (1986) 1003. https://doi.org/10.1021/ed063p1003.